Surface & Coatings Technology 205 (2011) 5502–5509

Contents lists available at ScienceDirect

Surface & Coatings Technology

journal homepage: www.elsevier.com/locate/surfcoat

Effect of annealing on the microstructure and erosion performance of cold-sprayed FeAl intermetallic coatings

Guan-Jun Yang, Hong-Tao Wang, Chang-Jiu Li *, Cheng-Xin Li

State Key Laboratory for Mechanical Behavior of Materials, School of Materials Science and Engineering, Xi'an Jiaotong University, Xi'an, Shaanxi, 710049, China

ARTICLE INFO

Article history:
Received 21 March 2011
Accepted in revised form 14 June 2011
Available online 25 June 2011

Keywords:
FeAl
Intermetallics
Cold spray
Annealing treatment
Solid particle erosion
Cohesion

ABSTRACT

FeAl intermetallic coatings were prepared by cold spraying of mechanically alloyed metastable Fe(Al) powder assisted with post-spray annealing treatment. The microstructure evolution and erosion performance of the coatings annealed at different temperatures were investigated and the erosion mechanism of the intermetallic coatings was examined through the surface morphology and cross-sectional microstructure of the eroded coatings. After annealing at 650 °C, the heterogeneous feature in the as-sprayed coating was evidently modified. With annealing temperature rising to 950 °C and 1100 °C, the interfaces between the particles in the coating completely disappeared. The erosion rate of the coating at the erosion angles of both 30° and 90° decreased with the increase in the annealing temperature. It was found that the erosion resistance of the intermetallic coating annealed at 1100 °C was three times higher than that of the as-sprayed coating. The weight loss of the as-sprayed coating with low cohesion at erosion angle of 90° was attributed to particle spalling off. The weight loss of the annealed intermetallic coatings with enhanced cohesion was attributed to microcutting and ploughing of erosive particles.

1. Introduction

Iron-aluminide intermetallic compounds have been proposed as one of the promising engineering materials for high temperature applications because of high specific strength and excellent corrosion resistance under oxidizing, sulfidizing atmospheres [1–3]. The high hardness, strength, and work hardening ability also make them be able to perform well in a variety of wear environments, such as wear and oxidation resistant parts in steelmaking industry [4–7]. Furthermore, these materials are competitive with most conventional ferrous alloys in terms of economic cost of raw materials, because they consist primarily of abundant and inexpensive elements (iron and aluminum). Thus, iron-aluminides have been considered for a variety of wear applications [8–12]. However, industrial applications of iron aluminides have been very limited owing to their low room temperature ductility and poor creep resistance [3]. Some studies have indicated that coating structural materials with iron aluminides using thermal spraying would not only solve the problems met in the fabrication of them into useful shapes, but also allow the effective use of their environment and corrosion resistant features [13–20]. However, the oxidation of the feedstock materials occurs during the conventional thermal spraying in which the feedstock undergoes a fully or partially melting state [16–20], which would change the compositions and microstructure of the feedstock and consequently degrade the properties of the deposits. Musalek et al. reported that, during fatigue service, the plasma-sprayed FeAl coatings fails due to the intersplat decohesion resulting from the nonbonded area and oxides layers between the lamellae [14,20].

Recently, cold spraying, as an emerging coating process, has been widely investigated owing to its capability to deposit many highly pure metallic or composite coatings [21–23]. In this process, feedstock particles (typically 5–45 μm) are accelerated to a high velocity (300–1200 m/s) by a supersonic gas jet generated through converging-diverging Laval type nozzle. A deposit is formed through the intensive plastic deformation of particles upon impact in a solid state at a temperature well below the melting point of the feedstock. Consequently, the deleterious effects inherent to conventional thermal spraying, such as oxidation, phase transformation and decomposition, can be minimized or eliminated [21]. This low temperature characteristic, as well as high deposition rate and relatively low cost, makes cold spraying as a promising process to fabricate FeAl intermetallic deposit with high performance. Due to the intrinsic brittleness of FeAl intermetallics at low temperature, it is difficult to deposit dense FeAl intermetallic coating directly using the FeAl intermetallic feedstock powder, because the insufficient deformation of the powder particles results in large pores in the coating even for high velocity oxy-fuel spraying [14,17,24,25]. For such intermetallic compound materials with the intrinsic low temperature brittleness, the coating process has been developed as cold spraying a pseudo-alloy with a designed element atomic ratio corresponding to a certain intermetallic compound, followed by post-spray annealing [26]. It was found that the phase structure in the feedstock can be retained in the as-deposited coating

* Corresponding author at: School of Materials Science and Engineering, Xi'an Jiaotong University, Xi'an, Shaanxi, 710049, China. Tel.: +86 29 82660970; fax: +86 29 83237910.
E-mail address: licj@mail.xjtu.edu.cn (C.-J. Li).

0257-8972/$ – see front matter © 2011 Elsevier B.V. All rights reserved.
doi:10.1016/j.surfcoat.2011.06.033

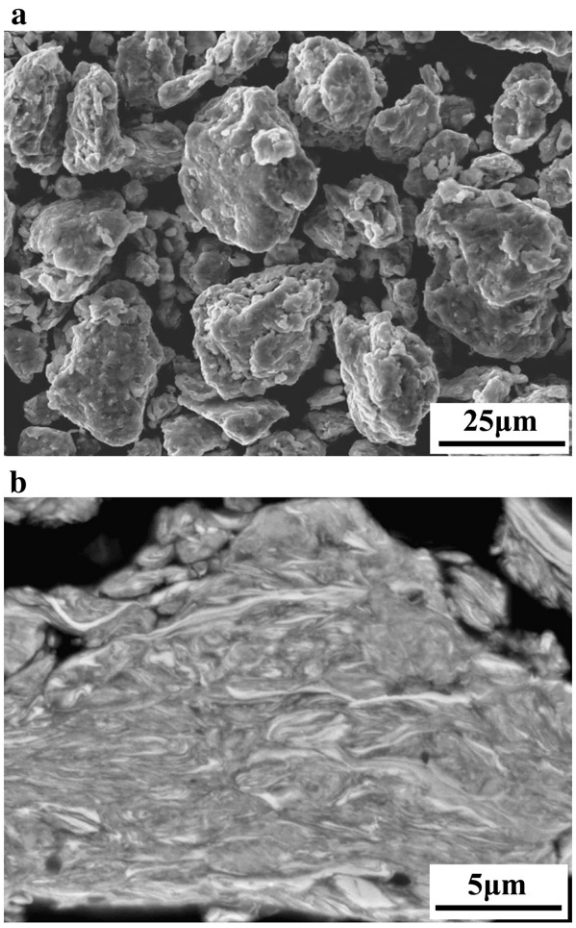

Fig. 1. Surface morphology (a) and cross-sectional microstructure (b) of the as-milled powder.

and nanostructured FeAl intermetallics can be evolved during post-spray annealing treatment in our previous study [26].

A cold-sprayed coating consists of the particles deformed to a lens-like shape. The orientation of deformed particles and the incompleteness of interface bonding between the deposited particles may result in the anisotropic coating microstructure and the low particle cohesion in the coating. Several reports [27–30] had demonstrated that the annealing treatment has significant effect on the microstructure and the properties of cold-sprayed coatings, such as releasing residual stress and decreasing porosity. Our previous result [26] showed that a cold-sprayed FeAl coating exhibits nanostructure, and therefore, it can be expected that the microstructure of cold-sprayed FeAl coating would be significantly modified through annealing treatment due to the low thermal stability of the nanostructure. Consequently, the performances of cold-sprayed FeAl coating, such as erosion wear resistance, would be also improved through annealing treatment.

In the present study, FeAl intermetallic coating was deposited by cold spraying. The effects of annealing treatment on the microstructure evolution and the erosion wear resistance of the coating were investigated. The erosion wear mechanism of the cold-sprayed FeAl intermetallic coatings was examined.

2. Experimental procedures

2.1. Materials

The commercially available Fe (99.8 wt.%, −54 μm, Youxinglian, Beijing, China) and Al (99.5 wt.%, −74 μm, Youxinglian, Beijing, China) powders were used as starting materials to produce a composite

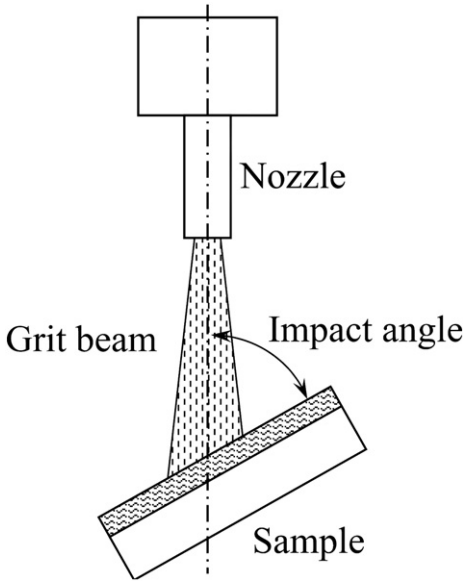

Fig. 2. Experimental setup for the erosion test.

feedstock powder with a composition corresponding to Fe60Al40 (molar ratio). The powder mixture was ball-milled in a high-energy ball mill, and a detailed description of the process was given elsewhere [26]. The powder milled for 36 h was sieved to a particle size less than

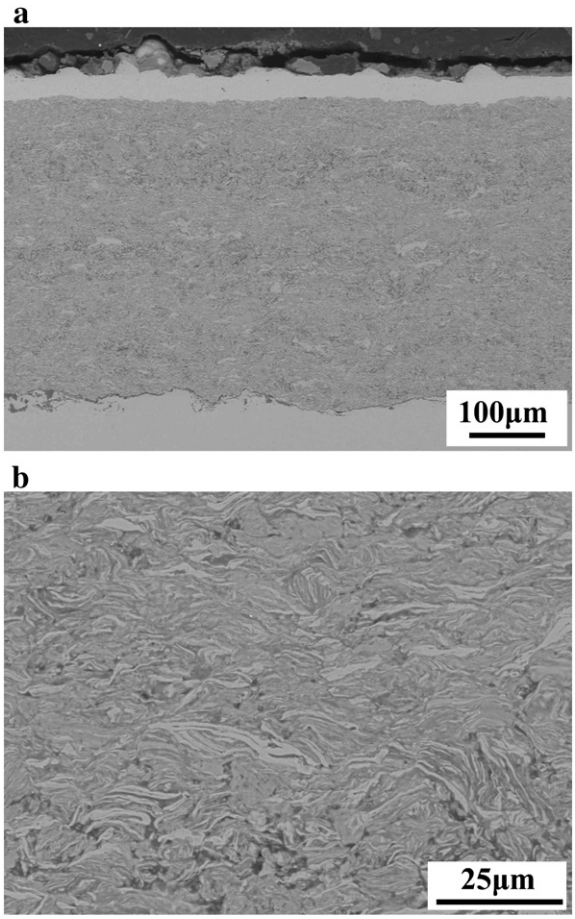

Fig. 3. Cross-sectional microstructure of the as-sprayed coating. (a) Low magnification, (b) high magnification. In Fig. 3a, the bottom white layer is substrate, the top white layer is electroless plated Ni, and the middle is the coating.

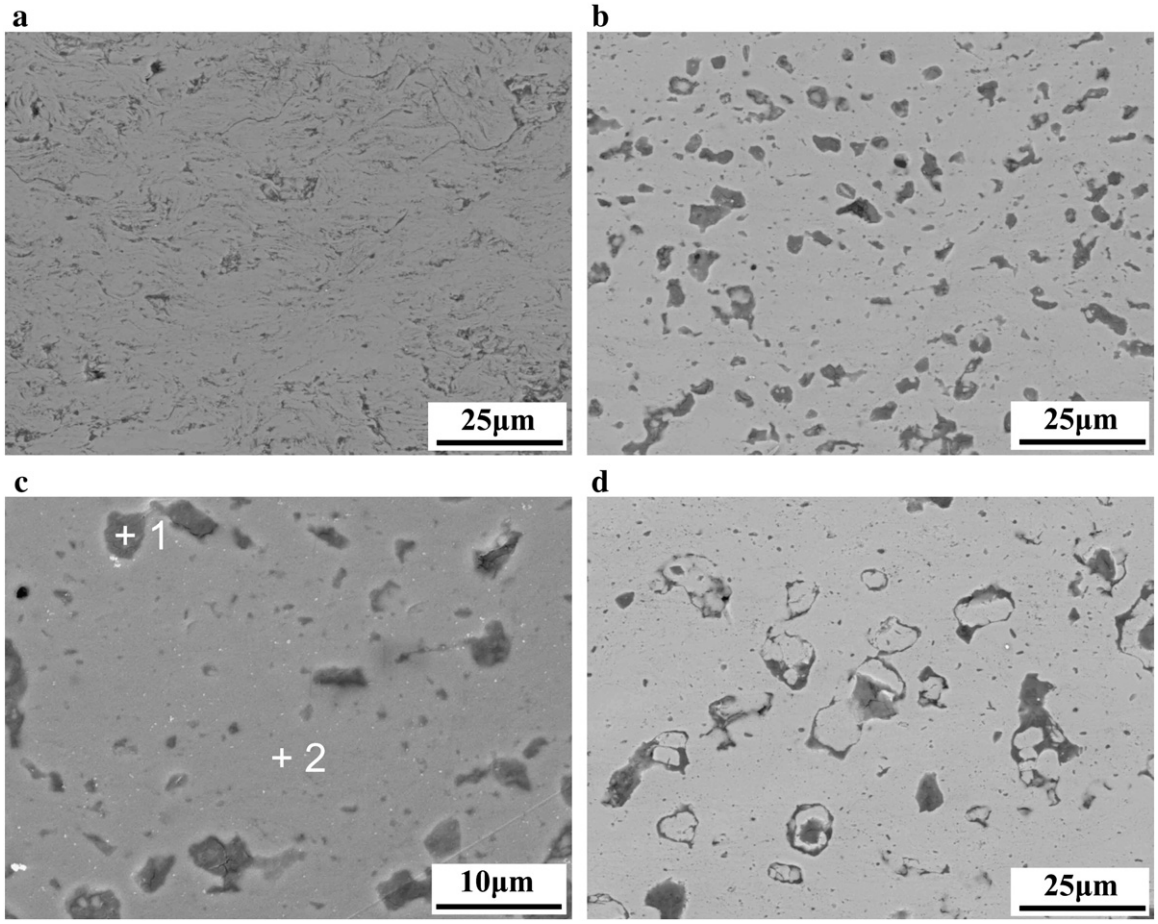

Fig. 4. Cross-sectional microstructure of the cold-sprayed coating annealed at different temperatures, (a) 650 °C, (b) (c) 950 °C and (d) 1100 °C.

Table 1
EDXA results of the points marked in Fig. 4c.

Positions	Fe K (at.%)	Al K (at.%)	O K (at.%)	Phase
Point 1	8.07	38.02	53.91	Al-rich oxide
Point 2	61.52	38.48	-	FeAl phase

45 μm and employed as the feedstock powder for spray deposition. Fig. 1 shows typical surface morphology and cross-sectional microstructure of the as-milled powder. The as-milled powder revealed the aggregation of layered Fe(Al) alloys showing an irregular angular morphology (Fig. 1a). As seen from the cross-sectional microstructure of the as-milled powder (Fig. 1b), a fine lamellar structure was present in the powder. Two distinguishable regions with different contrast can be clearly seen. A previous paper [26] suggested that the as-milled powder is Fe(Al) solid solution. The white layer is a Fe-rich phase, and the gray refined lamella is a Fe–Al solid solution with high Al content [26]. In cold spray process, the particle deposition takes place in a solid state, and consequently, this lamellar structure of the milled powder will be completely retained into the coating, giving a unique effect on the microstructure and the properties of the cold-sprayed coating. A low carbon steel (Q235) was used as a substrate for the deposition of FeAl coating. The substrate

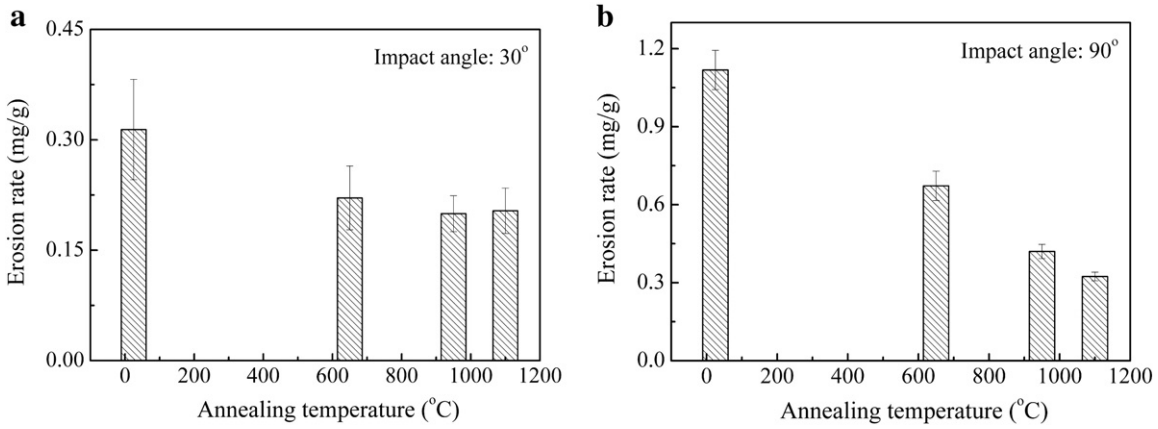

Fig. 5. Effect of annealing temperature on the erosion rate of the cold-sprayed FeAl coating at the impact angles of 30° (a) and 90° (b).

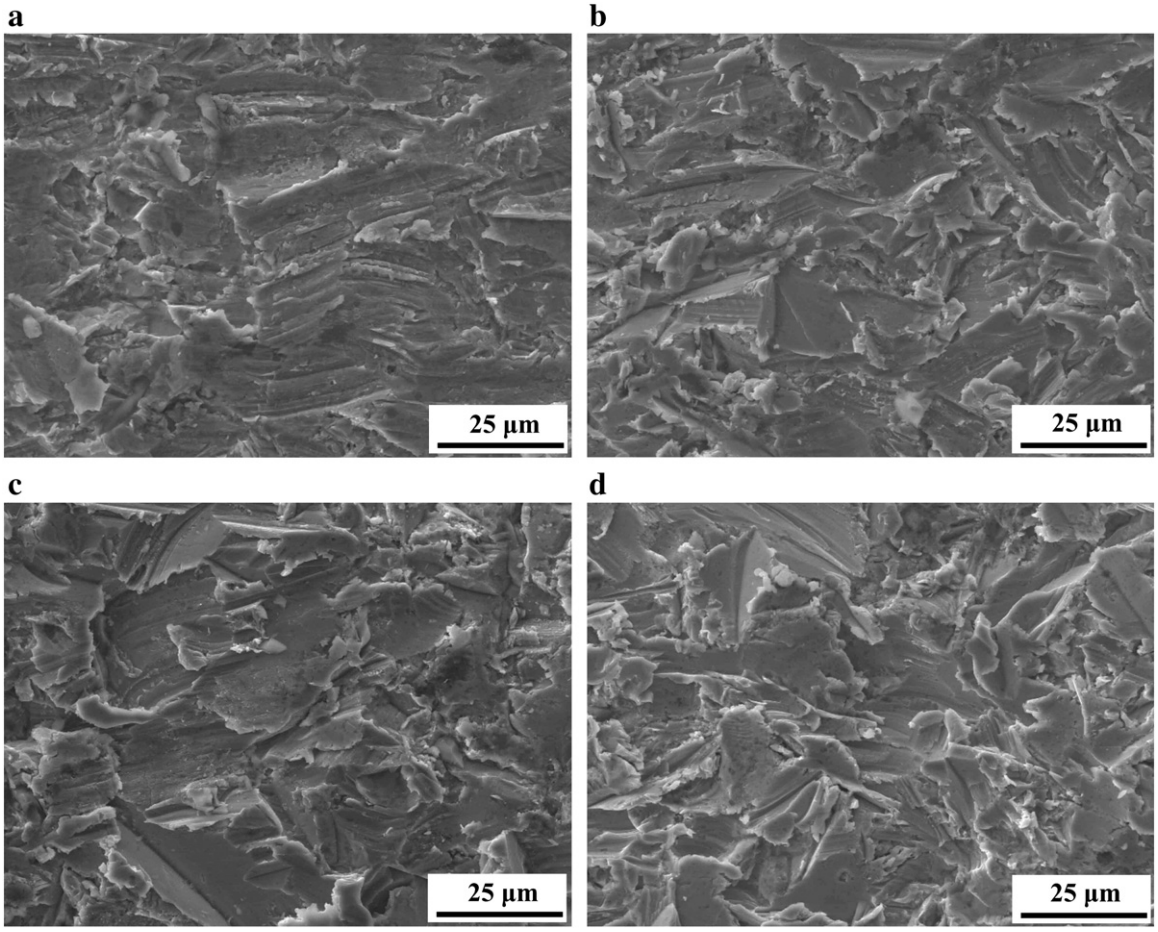

Fig. 6. Surface morphologies of the as-sprayed (a) and the coatings annealed at 650 °C (b), 950 °C (c) and 1100 °C (d) after erosion test at an impact angle of 30°.

surface was sand-blasted using 24 mesh alumina grits before coating deposition to improve the coating/substrate adherence.

2.2. Deposition of the coating

Fe–Al coating was deposited by a CS-2000 cold spray system (Xi'an Jiaotong University), the detailed description of which was given elsewhere [22]. A spray gun with a converging–diverging Laval type nozzle with a throat diameter of 2 mm was adopted. Nitrogen was used as both accelerating and powder feeding gases at 2.0 MPa and 2.5 MPa, respectively, and 510 °C in the pre-chamber. The standoff distance from the nozzle exit to substrate surface was 15 mm. During deposition, the spray gun was manipulated by a robot at a traverse speed of 40 mm/s relative to the substrate. In order to investigate the effect of annealing on the microstructure evolution and the erosion rate of cold-sprayed coating, the as-sprayed coating was annealed at 650 °C, 950 °C and 1100 °C for 5 h in an argon atmosphere at a heating and cooling rate of 10 °C/min.

2.3. Characterization of microstructure and cohesion

The surface morphology and the cross-sectional microstructure of the as-sprayed and the annealed coatings after erosion test were examined using scanning electron microscope (SEM) (Quanta 200, FEI, the Netherlands) equipped with energy dispersive X-ray analysis (EDXA). The cohesion of the coatings was measured by tensile test following ASTM C-633 standard at a cross-head speed of 1 mm/min. An epoxy (E-7 model, Shanghai Resin Research Institute, Shanghai, China) with an adhesive strength of 60 MPa was used in the test.

2.4. Erosion test

The erosion performance of the cold-sprayed FeAl coating was tested by a blast erosion tester as shown schematically in Fig. 2. A compressed air was used as an accelerating gas of erosive particles. In this tester, an accelerating nozzle has a diameter of 3.6 mm and a length of 22 mm. The pressure and the flow rate of the compressed air were set to 0.35 MPa and 141 L/min, respectively. Alumina grit with a nominal size of 250 μm was employed as the erodent. The impact angles during test were set to 30° or 90°. The distance from the nozzle exit to the center of sample surface was 100 mm to permit all erosive particles to impact on coating surface. The velocity of the alumina particles when impacting on the coating surface was about 60 m/s. The erosion test was performed with 20 g abrasives at one test and the total weight loss of the coatings was measured after each test. The erosion rate was estimated based on the linear relation between the total weight loss of the coatings and the weight of the abrasives used at a stable erosion state, and determined by the average value of five tests.

3. Results and discussion

3.1. Microstructure of the as-sprayed coating

The typical microstructure of the as-sprayed coating is shown in Fig. 3. The coating thickness was about 400 μm and the coating was well adhered to the substrate. The microstructure at a high magnification shown in Fig. 3(b) revealed that the coating had a dense microstructure and some thick white layers appeared in the coating microstructure. According to the X-ray diffraction and EDXA results in the previous paper [26], the as-sprayed coating consisted of

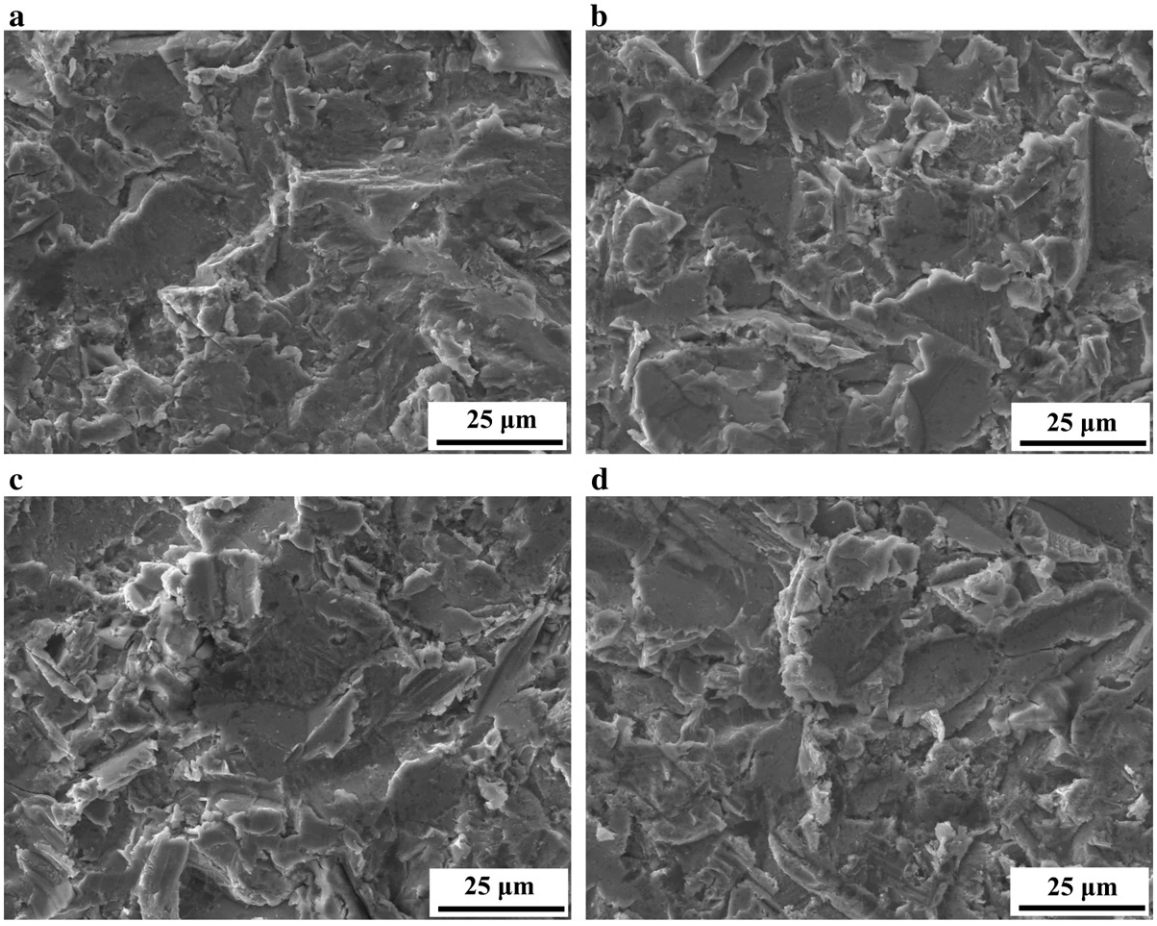

Fig. 7. Surface morphologies of the as-sprayed (a) and the coatings annealed at 650 °C (b), 950 °C (c) and 1100 °C (d) after erosion test at an impact angle of 90°.

Fe(Al) solid solution. The white layer was a Fe-rich phase, and the fine lamella was a Fe–Al solid solution with high Al content [26]. This indicated that the lamellar structure of the as-milled powder was completely retained into the coating. Moreover, from Fig. 3b, it was found that the coating presented a fine lamellar microstructure, which was similar to the lamellar structure in the feedstock powder shown in Fig. 1b. This indicated that the microstructure of the feedstock was well retained into the coating by cold spraying process. Compared to the clear particle/particle interface distinguished in the cold-sprayed coatings using the non-milled (metallic) powder mixture such as, the blends of Ni/Al powders [31] or Ti/Al powders [32], the particle/particle interface in the present cold-sprayed coating can not be clearly identified, since the particle/particle interface morphology is similar to that in the fine lamellar microstructure of the feedstock. Therefore, it was difficult to distinguish a single deformed particle and the particle boundary in the coating.

3.2. Effect of annealing on the microstructure

The cross-sectional microstructures of the cold-sprayed coatings annealed at 650 °C, 950 °C and 1100 °C were shown in Fig. 4. To reveal the microstructure evolution, the microstructures of the annealed coatings were all examined in the back-scattered electron mode. It was clearly seen that the microstructure of the cold-sprayed coating significantly changed after annealing at these temperatures. After annealing at 650 °C, white Fe-rich zones and fine lamellae in the as-sprayed coating (Fig. 3) disappeared due to the possible element diffusion within the coating, as shown in Fig. 4a. When the annealing temperature was raised to 950 °C, the lamellar microstructure in the coating completely disappeared, which would be beneficial to improve both the cohesive and the adhesive strength, as shown Fig. 4b and c. The similar result was also observed in the annealing treatment of cold-sprayed FeAl/Al_2O_3 composite [33]. This means that the heterogeneous feature in the as-sprayed coating can be modified by post-spraying annealing treatment. However, some dark particles appeared in the coating, which was Al-rich oxide, being confirmed by EDXA results as shown in Table 1. It is possibly due to the growth of the oxide in the as-sprayed coating during annealing treatment [34]. With raising annealing temperature to 1100 °C, the microstructure of the coating exhibited no evident change compared to that of the coating annealed at 950 °C, except that oxide particles in the coating became larger due to high temperature. This indicated that the annealing treatment at 950 °C was sufficient to significantly improve the cohesion of the cold-sprayed FeAl coatings.

To further quantitatively reveal the effect of annealing on the cohesion of the cold-sprayed FeAl coatings, the tensile test of the coatings was performed according to ASTM C633 standard. The coating was firstly tested and the adhesive strength was obtained, because the fracture occurred at the interface between the coating and substrate. Then, the sample with the coating was glued to another coupling sample with the adhesives, and the tensile test was performed again. Results showed that the cohesion strength of the coating was 38 ± 4 MPa in the as-sprayed state and was increased to 46 ± 5 MPa after the annealing at 650 °C. When the annealing temperature was higher than 950 °C, the fracture occurred within the adhesives. This means that the cohesive strength of the coatings became higher than the strength of the adhesives, which was 60 ± 6 MPa in this study. Therefore, those results were consistent with the observation on the microstructure of the coatings.

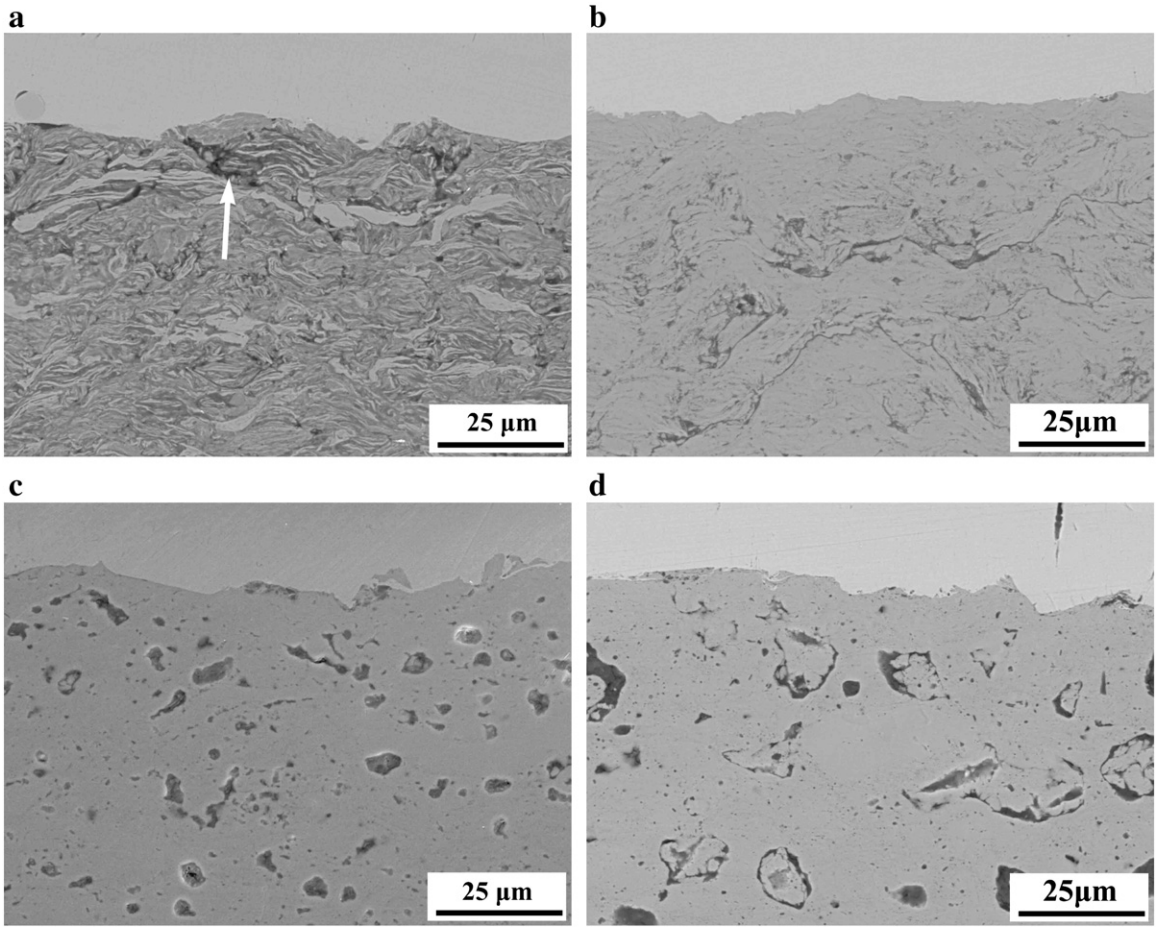

Fig. 8. Cross-sectional microstructure of the as-sprayed (a) and the coatings annealed at 650 °C (b), 950 °C (c), 1100 °C (d) after erosion test at an impact angle of 30°.

3.3. Effect of annealing on the erosion performance

Fig. 5 shows the effect of annealing temperature on the erosion rate of the cold-sprayed FeAl coating. It can be seen that the erosion rate was decreased with the increase in the annealing temperature at the impacting angles of both 30° and 90°. This indicated that annealing treatment can significantly improve the erosion resistance of the cold-sprayed FeAl coating. The erosion rate of the as-sprayed coating at 30° was 0.31 mg/g, and after annealing at 650 °C, the erosion rate decreased to 0.21 mg/g, as shown in Fig. 5a. This can be attributed to the different phase structure of the as-sprayed coating from that of the coating annealed at 650 °C. The as-sprayed coating was Fe(Al) solid solution. However, the phase of the coating annealed at 650 °C changed into FeAl intermetallic compound [26]. It was well known that FeAl intermetallic compound presents excellent wear resistance due to its high strength and work hardening ability [4]. Therefore, the FeAl intermetallic coating annealed at 650 °C showed a relatively low erosion rate compared to as-sprayed Fe(Al) alloy coating. In addition, it can also be found that the erosion resistance of the coatings annealed at a temperature above 650 °C was little influenced by the annealing temperature, since all those coatings had been transformed into intermetallics from the metallic phases in the feedstock. From Fig. 5b, it can be clearly seen that the erosion resistance of the cold-sprayed FeAl coating at 90° increased with the increase in annealing temperature. The erosion rate of the as-sprayed coating at 90° was 1.12 mg/g. With raising annealing temperature, the erosion rate of the coating continuously decreased. After annealing at 1100 °C, the erosion rate of the coating significantly decreased to 0.32 mg/g, which was less than one third of that of the as-sprayed coating. It was reported that the erosion rate of the coating at 90° reflects the bonding state of laminate structure in the coating [35,36]. Therefore, this result indicated that the bonding at the interfaces between deposited particles in the cold-sprayed FeAl coating was significantly improved with raising annealing temperature. The erosion test result was consistent with the change of microstructure of the annealed coating observed in Section 3.2. In addition, comparing the results in Fig. 5a and b, it is clear that the erosion rate of the cold-sprayed FeAl coating at 90° after annealing at different temperatures was always higher than that of corresponding coating at 30°. This is because FeAl intermetallic compound is brittle at low temperature [3]. According to the erosion theory of brittle materials, the erosion rate becomes the maximum at an impact angle of about 90°, since the material loss at high impact angles is dominated by the impact-induced cracking and the subsequent flaking off rather than micro-cutting [37]. It will decrease with the decrease in impact angle. Therefore, the present test results confirm the brittle characteristics of FeAl coating at room temperature.

3.4. Effect of annealing on the erosion behavior

The surface morphologies of the as-sprayed coating and the annealed cold-sprayed FeAl coatings at 650 °C, 950 °C, and 1100 °C after erosion test at impact angles of 30° and 90° were shown in Fig. 6 and Fig.7, respectively. Many narrow ploughs were observed on the surface of the coating eroded at an impact angle of 30° (Fig.6), and only a small amount of craters existed on the eroded surface. Those narrow ploughs were formed through the cutting by alumina erosive particles. On the contrary, when erosion test was performed at 90°, many craters were observed and few ploughs were observed on the eroded coating surface, as shown in Fig. 7. This is because the cutting effect of erosive

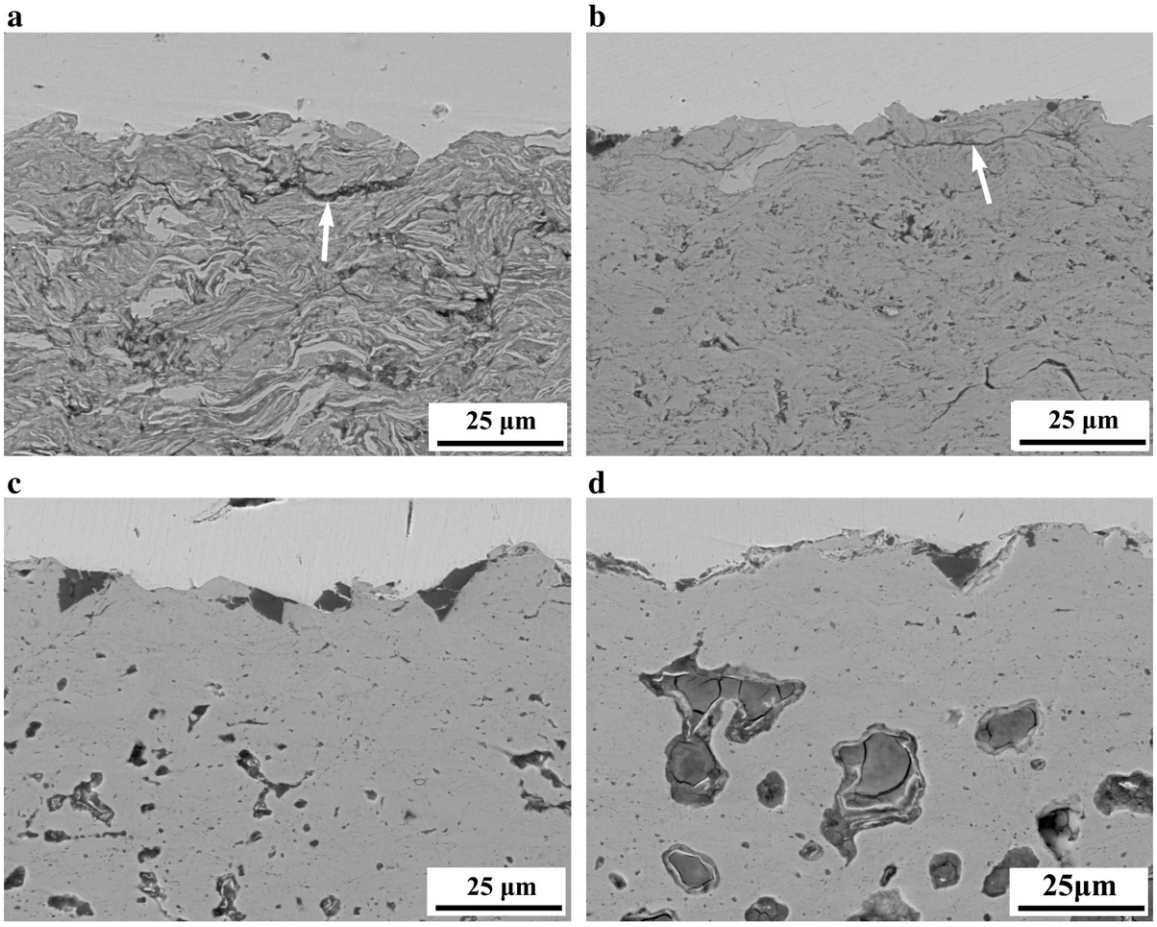

Fig. 9. Cross-sectional microstructure of the as-sprayed (a) and the coatings annealed at 650 °C (b), 950 °C (c), 1100 °C (d) after erosion test at an impact angle of 90°.

particles decreases and impact effect correspondingly increases with changing the erosive angle from 30° to 90°. Based on this observation, the little influence of annealing temperature on the erosion rate of the coating at a temperature above 650 °C at an impact angle of 30° is possibly attributed to the similar intrinsic anti-cutting resistance of those coatings, since all those coatings were composed of FeAl intermetallics.

Figs. 8 and 9 show the cross-sectional microstructure of the as-sprayed and the annealed coatings after erosion test at impact angles of 30° and 90°, respectively. Large cracks along lamellar interface, marked by white arrows, can be clearly seen near the coating surface after the as-sprayed coating was subjected to erosion, as shown in Figs. 8a and 9a. Cracks, which initiate at and propagate along the lamellar interfaces under the impact of erosive particles, are due to the limited bonding at the particle interfaces. Cold-sprayed coating was formed through the intensive plastic deformation of particles upon the impact in a solid state at a temperature well below the melting point of the spray material. Therefore, the adjacent two particles were bonded weakly, and the nonbonded interface area existed between the particles [22,38–42]. The nonbonded interface area will act as a pre-crack, which propagates under the impact of erosive particles on the coating surface. Consequently, before the particle is completely ploughed by erosive particles, the crack propagation originating from the nonbonded interface area may lead to spalling off of one particle or multiple particles, which were exposed on coating surface and subjected to the direct impact of erosive particles. Therefore, it can be considered that the crack propagation along weakly bonded lamellar interface and the subsequent spalling-off of particle would be the dominant erosion mechanism of the as-deposited coating with low cohesion especially at the impact angle of 90°. For the coating annealed at 650 °C, cracks were also observed near the coating surface when the impact angle was 90°, as shown in Fig. 9b. This indicates that the cohesion between the particles in the coating was still not sufficiently enhanced. With raising annealing temperature to 950 °C and 1100 °C, no evident cracks were observed near the coating subsurface after erosion test, as shown in Fig. 8c–d and Fig. 9c–d. This indicates that the cohesive strength between particles had been significantly improved through the annealing treatment at 950 °C. This result is in consistence with the observation results on the microstructure evolution of the coating during annealing treatment in Section 3.2 and the cohesion test results of the coating as mentioned previously as well. Therefore, for the coatings annealed at a temperature higher than 950 °C, the dominant erosion mechanism during erosion test will be microcutting and ploughing by erosion particle. As a result, the erosion wear resistance of the annealed coating at 30° was almost the same when the annealing temperature was from 650 to 1100 °C. Compared the erosion rate of the coating annealed at 650 °C with those of the coatings annealed at 950 °C and 1100 °C at the impact angle of 30°, although a significant improvement in the particle cohesion within the coating was recognized, the erosion rate was not significantly reduced. This indicates that at the erosion angle of 30°, although cracking along the lamellar interface was observed, the effect of such cracking on the erosion of the coating was limited. The dominant erosion mechanism at the impact angle of 30° is microcutting and ploughing.

4. Conclusions

FeAl intermetallic compound coating was deposited by cold spraying. The effect of annealing treatment on the microstructure

and the erosion performance of cold-sprayed FeAl coating was investigated. Results showed that the as-sprayed coating had a lamellar microstructure. When annealing the coating at 650 °C, the heterogeneous feature in the as-sprayed coating was evidently modified. When the annealing temperature increased to 950 °C and 1100 °C, the interfaces between the particles in the coating completely disappeared due to element diffusion. The erosion performance of the cold-sprayed FeAl coating was significantly influenced by annealing treatment. The erosion rate of the cold-sprayed coating at the erosion angles of both 30° and 90° decreased with the increase in the annealing temperature. The weight loss of both the as-sprayed coating and the annealed FeAl coatings at the erosion angle of 30° was mainly attributed to microcutting and ploughing of erosive particles. At the erosion angle of 90°, the weight loss of both the as-sprayed coating and the FeAl coating annealed at 650 °C was attributed to particle spalling off from the surface. The erosion of the coating annealed at 950 and 1100 °C was attributed to microcutting and ploughing of erosive particles. It was found that the erosion resistance of the coating annealed at 1100 °C was three times higher than that of the as-sprayed coating owing to the significant enhancement of interface bonding by annealing treatment.

Acknowledgements

The present work is supported by the National Science Foundation for the Distinguished Young Scholars (No. 50725101), Key Project of the Ministry of Education of China (No. 106145), and Program for New Century Excellent Talents in University (No. NCET-08-0443).

References

[1] N.S. Stoloff, Mater. Sci. Eng. A 258 (1998) 1.
[2] Y. Wang, W. Chen, Surf. Coat. Technol. 183 (2004) 18.
[3] S.C. Deevi, V.K. Sikka, Intermetallics 4 (1996) 357.
[4] M. Krasnowski, T. Kulik, Intermetallics 15 (2007) 201.
[5] C.T. Liu, E.P. George, P.J. Maziasz, J.H. Schneibel, Mater. Sci. Eng. A 258 (1998) 84.
[6] J. Yang, P. La, W. Liu, Q. Xue, Wear 257 (2004) 104.
[7] A.Y. Mosbah, D. Wexler, A. Calka, Wear 258 (2005) 1337.
[8] G. Ji, T. Grosdidier, F. Bernard, S. Paris, E. Gaffet, S. Launois, J. Alloys Compd. 434–435 (2007) 358.
[9] L. D'Angelo, L. D'Onofrio, G. Gonzalez, J. Alloys Compd. 483 (2009) 154.
[10] R. Subramanian, J.H. Schneibel, Intermetallics 5 (1997) 401.
[11] J.P. Tu, L. Meng, M.S. Liu, Wear 220 (1998) 72.
[12] D.E. Alman, J.A. Hawk, J.H. Tylczak, C.P. Dogan, R.D. Wilson, Wear 251 (2001) 875.
[13] S.-C. Wei, B.-S. Xu, H.-D. Wang, G. Jin, H. Lv, Surf. Coat. Technol. 201 (2007) 6768.
[14] C. Xiao, W. Chen, Surf. Coat. Technol. 201 (2006) 3625.
[15] Z.Y. Liu, W. Gao, F.H. Wang, Scripta Mater. 39 (1998) 1497.
[16] C. Senderowski, Z. Bojar, W. Wo1czynski, A. Paw1owski, Intermetallics 18 (2010) 1405.
[17] J.M. Guilemany, C.R.C. Lima, N. Cinca, J.R. Miguel, Surf. Coat. Technol. 201 (2006) 2072.
[18] S. Frangini, A. Masci, Surf. Coat. Technol. 184 (2004) 31.
[19] G. Ji, O. Elkedim, T. Grosdidier, Surf. Coat. Technol. 190 (2005) 406.
[20] R. Musalek, O. Kovark, T. Skiba, P. Hausild, M. Karlk, J. Colmenares-Angulo, Intermetallics 18 (2010) 1415.
[21] A. Papyrin, Adv. Mater. Process 159 (2001) 49.
[22] C.-J. Li, W.-Y. Li, Surf. Coat Technol. 167 (2003) 278.
[23] R.S. Lima, J. Karthikeyan, C.M. Kay, J. Lindemann, C.C. Berndt, Thin Solid Films 416 (2002) 129.
[24] G. Ji, T. Grosdider, H.L. Liao, J.-P. Morniroli, C. Coddet, Intermetallics 13 (2005) 596.
[25] T. Grosdidier, G. Ji, F. Bernard, E. Gaffet, Z.A. Munir, S. Launois, Intermetallics 14 (2006) 1208.
[26] H.-T. Wang, C.-J. Li, G.-J. Yang, C.-X. Li, Q. Zhang, W.-Y. Li, J. Therm Spray Technol. 16 (2007) 669.
[27] C. Borchers, F. Gärtner, T. Stoltenhoff, H. Kreye, Acta Mater. 53 (2005) 2991.
[28] W.-Y. Li, C.-J. Li, H.-L. Liao, J. Therm Spray Technol. 15 (2006) 206.
[29] R.C. McCune, W.T. Donlon, O.O. Popoola, E.L. Cartwright, J. Therm Spray Technol. 9 (2000) 73.
[30] X.-J. Ning, J.-H. Kim, H.-J. Kim, C. Lee, Appl. Surf. Sci. 255 (2009) 3933.
[31] H.Y. Lee, S.H. Jung, S.Y. Lee, K.H. Ko, Appl. Surf. Sci. 253 (2007) 3496.
[32] T. Novoselova, S. Celotto, R. Morgan, P. Fox, W. O'Neill, J. Alloys Compd. 436 (2007) 69.
[33] H.-T. Wang, C.-J. Li, G.-J. Yang, C.-X. Li, Vacuum 83 (2008) 146.
[34] K. Wolski, F. Thevenot, J. Coze, Intermetallics 4 (1996) 299.
[35] C.-J. Li, G.-J. Yang, A. Ohmori, Wear 260 (2006) 1166.
[36] Y. Wang, M. Yan, Wear 261 (2006) 1201.
[37] P.A. Engel, Impact Wear of Materials, Elsevier, Amsterdam, 1976.
[38] G. Bae, S. Kumar, S. Yoon, K. Kang, H. Na, H.-J. Kim, C. Lee, Acta Mater. 57 (2009) 5654.
[39] T. Hussain, D.G. McCartney, P.H. Shipway, D. Zhang, J. Thermal Spray Technol. 18 (2009) 364.
[40] K. Ogawa, K. Ito, K. Ichimura, Y. Ichikawa, S. Ohno, N. Onda, J. Thermal Spray Technol. 17 (2008) 728.
[41] T.S. Price, P.H. Shipway, D.G. McCartney, E. Calla, D. Zhang, J. Thermal Spray Technol. 16 (2007) 566.
[42] M. Grujicic, J.R. Saylor, D.E. Beasley, W.S. DeRosset, D. Helfritch, Appl. Surf. Sci. 219 (2003) 211.